Low Earth Orbit Plasma Wake Shaping and Applications to On-Orbit Proximity Operations

Jordan Maxwell and Hanspeter Schaub

***Abstract*—A parametric investigation of plasma wake geometry is conducted to determine the applicability of Coulomb actuation to resident space objects (RSO) in low Earth orbit (LEO). The use of Coulomb forces could provide a touchless means to achieve relative position and attitude adjustments between close-proximity objects on orbit. Theoretical models developed for techniques in the Geosynchronous Earth Orbit (GEO) regime indicate that Coulomb actuation could facilitate on-orbit proximity operations in a highly fuel- and power-efficient manner. In LEO however, only the plasma parameters in the wakes behind orbiting objects are a promising region for Coulomb actuation applications. These physical phenomena investigated by the Charging Hazards And Wake Studies (CHAWS), Space Experiments with Particle Accelerators (SEPAC), and other on-orbit experiments exhibit substantially decreased plasma density relative to ambient. This investigation considers the wake which forms behind objects of various potentials and cross sectional areas, particularly focusing on methods of enhancing the wake with negligible changes in the objects area and, therefore, mass. Experimental results are presented and compared with previous theoretical, numerical, and experimental work. The size of a wake formed by an uncharged object is shown to depend on its cross-sectional area. However, the same object charged to a positive potential generates a substantially larger wake. Additional experimental results indicate that a positively charged, sparse structure with similar dimensions but significantly less cross-sectional area forms a wake similar to the previous, solid object charged to the same level. This indicates that a large wake can be generated without significantly increasing mass or area-dependent perturbations such as drag and solar radiation pressure. These results increase the applicability of Coulomb actuation in LEO by enhancing the region in which the technique is feasible.**

***Index Terms*—Plasma, Plasma Wakes, Wake Shaping, Space Physics.**

I. Introduction

Spacecraft charging has been a subject of study for the past several decades. Until recently, the potential hazards and charging mitigation strategies have been the primary focus of this work. This paper builds on the growing body of research investigating the use of charge accumulation on spacecraft surfaces to accomplish relative positions and attitudes between two RSOs. This technique, called electrostatic actuation, [1], [2] has the key benefits of being touchless, using virtually no fuel, and being capable of despinning an object — a capacity that conventional capture methods lack. [3]–[5] Several applications have been developed for objects in Geostationary Earth Orbit (GEO), but until recently it was assumed that the cold, dense plasma characteristic of much of the ionosphere would prove prohibitive to LEO electrostatic actuation applications. However, the relatively sparse plasma in the wakes that form behind objects orbiting in LEO exhibit plasma parameters conducive to the technique. [6] The work presented here investigates various methods for expanding the wake region to facilitate electrostatic actuation as illustrated in Figure 1.

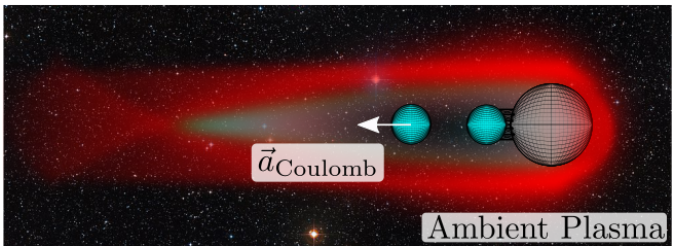

Fig. 1. Electrostatic Actuation in LEO Plasma Wakes

Wakes form behind orbiting objects in LEO because the orbital velocity is supersonic with respect to the plasma ions and neutrals. This creates a region antiparallel to the object's velocity that is nearly devoid of these species [7]. Electrons, which have extremely low mass, move much more rapidly and are therefore able to penetrate into the wake. However, the lack of ions in this region creates a negative space charge which screens out lower-energy electrons, so the electron density is decreased and the temperature increased as shown by [8] and [9], respectively.

A substantial body of research describing LEO plasma wakes exists. References [10], [11] numerically model wake structures in LEO-like plasmas for objects of various sizes, geometries, and voltages, while [12], [13] use simulation chambers to analyze wake structures behind objects of different sizes, geometries, speeds, and voltages. Reference [14] presents a set of dimensionless parameters which describe how plasma-body interactions that generate the wake scale in LEO. A variety of missions have been conducted to analyze spacecraft charging and beam structures within LEO, including CHAWS [15] and SEPAC [16], the latter of which showed that objects in the wake can be charged to $\sim$ 5kV with a $\sim$ 800W electron gun. This indicates that, should the wake be sufficiently large to envelop a craft or object, electrostatic actuation can be applied to influence the relative positions and attitudes between the wake-forming craft and the follower. The sources listed above describe the plasma parameters in

Jordan Maxwell is a graduate research assistant at the University of Colorado at Boulder, (email: Jordan.Maxwell@Colorado.edu)

Hanspeter Schaub is a Professor and Glenn L. Murphy Chair of Engineering at the University of Colorado at Boulder, (email: Hanspeter.Schaub@Colorado.edu)

the wake in detail, but have not explored active wake shaping methods.

GEO applications for the use of electrostatics on-orbit have been the primary research focus because the plasma in this region is hot and sparse — prime conditions for charging and electrostatic force and torque propagation. The electrostatic tractor technique [17] employs an electron/ion beam to charge another orbiting body, generating electrostatic forces and torques for touchless interactions, much as in Figure 1. Proposed applications include space debris removal [18], [19], detumbling of rapidly rotating objects on orbit [17], orbital corrections [20], and electrostatically inflated gossamer structures [21]. Extension of such techniques to LEO requires that the wake region where electrostatic actuation is possible be large enough to envelop the follower.

The research presented here is also relevant to the burgeoning field of charged aerodynamics in the ionosphere. Reference [22] shows that, for certain orbits and surface potentials, the drag acceleration experienced by an RSO can be significantly larger than that at zero surface potential. Therefore, the drag acceleration can be controlled via modulation of the surface charge. This could facilitate de-orbiting operations, semi-major axis and eccentricity changes, and formation keeping in addition to the electrostatic actuation applications discussed above.

II. Experimental Methods

Plasma wake experiments were conducted within the JUMBO chamber at the Spacecraft Charging Instrumentation and Calibration Laboratory (SCICL) at the Air Force Research Laboratory (AFRL) at Kirtland Air Force Base, NM. JUMBO is a 1 m diameter cylindrical chamber with length of roughly 3 m and is described in greater detail in [23]. The plasma source manufactured by Plasma Controls LLC uses magnetic filtering to produce a representative LEO plasma — one in which the thermal velocity of the streaming, directional ions is roughly equivalent to the relative velocity of a LEO spacecraft with respect to ionospheric ions. Argon gas is ionized by a filament within the source to generate the ions which are then accelerated to the desired velocities by a system of charged grids. Argon is chosen because its mass is representative of the higher-concentration elements within the ionosphere and because Ar^+ is not as corrosive as elements such as O^+. This source is not differentially pumped, meaning that neutral Argon atoms are present within the flow, allowing for charge exchange between the fast-moving ions and the slow neutrals. The effect of this phenomenon is currently under investigation.

Figure 2 shows the experimental setup. The plasma source is on the left. In the center is a solid, conducting sphere of radius 10 cm about which the wake is generated. On the right is a Langmuir probe package affixed to a 3-dimensional translation stage. A measurement is taken at each point of a 3-dimensional grid beginning 1 mm behind the spherical conductor and extending for 6.5 cm. This provides a measurement of the wake. The I-V curve from the Langmuir probe is measured using a Keithley 6487 Source-Measure Unit (SMU). This model is capable of measuring currents on the order of femtoamps given the right equipment and conditions. However, given the experimental parameters and available equipment, the lowest reliably-measurable current was 10^{-8} A.

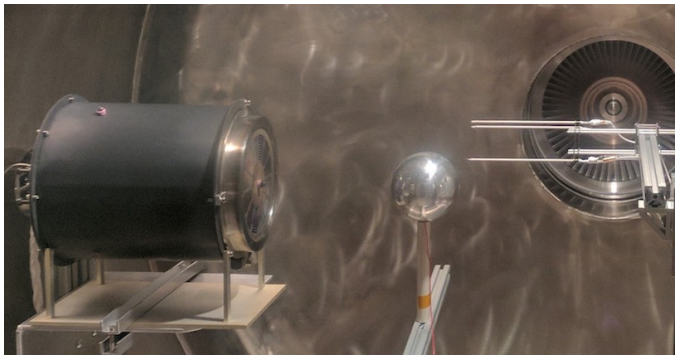

Fig. 2. Wake Experiment Setup

Four experiments were carried out to investigate the wake structure under various voltages and geometries. Table I provides the values used in these experiments.

TABLE I
Experiment Descriptions

Experiment	Applied Voltage (V)	Experiment Article
A	-1 (V_{Float})	Solid Conducting Sphere
B	-50	Solid Conducting Sphere
C	50	Solid Conducting Sphere
D	50	Sparse Conducting Sphere

Fig. 3. Sparse Sphere for Experiment D

All experiments were carried out at pressures below 10^{-4} Torr. The plasma source operating conditions are listed in Table II.

TABLE II
PLASMA SOURCE VOLTAGES & CURRENTS

Source Property	Value
$V_{Discharge}$ (V)	30-40
$I_{Discharge}$ (A)	0.9
V_{Keeper} (V)	15-20
I_{Keeper} (A)	1
Mass Flow Rate (sccm)	10

The parameters given in Table II generate a plasma with density of roughly 10^{14} m^{-3} and an electron temperature on the order of 0.1 eV. These properties reasonably match the calibration provided by Plasma Controls LLC. It is worth noting that, while the plasma source is expected it have directionally streaming ions at roughly 5 eV, no calibration is provided to validate this. Characterization of the source is an ongoing effort.

As seen in Figure 2, the plasma source is located at one end of the chamber and is aligned perpendicular to the axis of the chamber. Based on the Langmuir probe data collected, the grounded rear and side of the chamber are at roughly -1 V with respect to the plasma, meaning that the ions in the plasma flow are attracted to the walls, sides, and floor of the chamber, while the electrons are repelled. This is seen in the data shown in the next section.

Each Langmuir sweep taken throughout all experiments spans -10V to 10V with 50 equally spaced voltages at which current measurements are taken throughout each sweep. Each sweep runs from negative to positive. The integration time on the Keithley 6487 SMU is set to minimize the sweep time while maintaining enough accuracy to collect quality data. Each sweep takes less than one second and is separated from the previous sweep by the amount of time the 3-dimensional translation stage requires to move 1 cm to the next grid point — about 1 second. The floating potential on the charged conducting sphere was determined empirically using a non-contact electrostatic field probe (Trek model 341B).

III. DATA ANALYSIS

The Langmuir curves generated by the Keithley 6487 SMU are analyzed using the method described by [24] in which the 4-parameter fitting function shown in Equation (1) is fit to the data and used to extract the properties of the plasma.

$$I(V) = \exp\left[a_1 \tanh\left(\frac{V + a_2}{a_3}\right)\right] + a_4 \qquad (1)$$

Here, V is the probe potential and the a_i are the fitting parameters. This fitting method provides varying degrees of success, and the amount of data collected prohibits individual tuning of fit parameters. Figure 4 shows three examples of experimental data. Note that the RMS of the fit residuals is indicated within the caption on each figure.

Figure 4a shows a data set that is well described by Equation (1). The plasma properties extracted according to [24] for similar data sets are considered accurate as they match the calibrations done by Plasma Controls LLC. Figure 4b shows

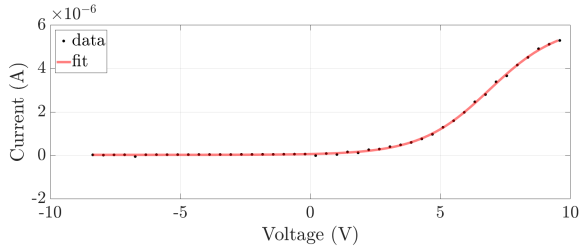

(a) Instance of Good Fit to Reliable Data (RMS=0.0063568)

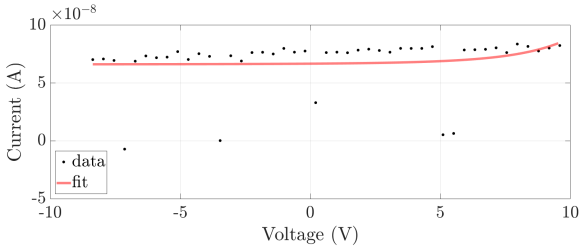

(b) Instance of Fit to Unreliable Data RMS = 0.26292)

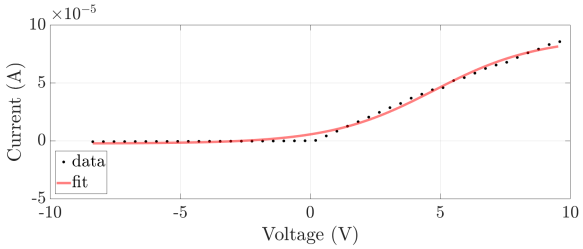

(c) Instance of Bad Fit to Reliable Data (RMS = 0.026656)

Fig. 4. Fits to Langmuir Probe Data

a case where the detector floor was hit, providing unreliable data that the model is nevertheless able to fit. These data sets are excluded from the results.

Due to the large amount of data collected, each fit cannot be considered individually. The RMS value provides a good means of identifying good fits from poor, but given that plasma properties are extracted from different voltage regimes within each Langmuir probe sweep, the RMS value does not provide the full picture. For example, a data set whose fit is good on the negative end of the I-V curve will provide an accurate measure of the ion density of the plasma, while that same fit may be poor in the positive regime and therefore provide inaccurate values for the electron density and temperature. This is seen in Figure 4c, as the fit is much better for negative voltage values than for those from roughly -1 V and above.

Additionally, the properties of the wake described previously — such as its non-quasi-neutral nature — mean that many of the assumptions outlined in [24] and other conventional Langmuir probe analyses are invalid. Future iterations of this work will investigate the use of different fitting and analysis methods to determine the plasma properties in the wake. This paper is primarily concerned with the feasibility of changing the wake geometry, rather than precise determination

of the wake properties.

IV. Results & Discussion

Each of the experiments outlined in Table I consist of a Langmuir probe sweep taken at the nodes of a 3-dimensional grid. Only the measured densities are considered in this section, as the fitting challenges discussed in the previous section especially affected the electron temperature measurement. Additionally, the wake is most recognized for the ion density decrease relative to ambient, so this geometrical investigation can continue without consideration of the electron temperature.

Each of the figures shown below is oriented as is the experiment in Figure 2 — with the plasma flowing from left to right. Additionally, a circle of radius equal to the radius of the conducting sphere is superimposed on the plots to show the size of the wake relative to the wake-forming object. The Z = 0cm plane shown on the far left of each of Figures 5-8 begins directly behind the charged conducting sphere, meaning that values surrounding the wake center at $[0,0,0]^{\mathrm{T}}$ are likely within the charged sphere's sheath, where the Langmuir probe analysis does not apply.

Note that each figure below shows the plasma density decreasing as the Z distance increases. This is because the plasma is expanding into the JUMBO chamber. This could affect the wake closure distance, but the detailed analysis required to understand this aspect of the experiment is not within the scope of this investigation. However, reference [25] provides a method of describing how the ambient plasma expands.

Finally, the ion-deficient nature of the wake means that shielding effects are asymmetric with respect to potential, as described in [26]. Therefore, the negative potentials applied to the Langmuir probe while in the wake could affect a significantly larger portion of the plasma than in ambient. Shielding effects are reduced in the positive regime as well, meaning that the sheath about the probe is larger, leading to increased current collection when the probe is charged positive. This could in part describe the electron density enhancements seen in the wake in the figures below. The short integration time discussed previously was used in part to mitigate this effect, but sampling on timescales less than the plasma frequency (roughly 10^8 Hz) was not possible with the Keithley 6487.

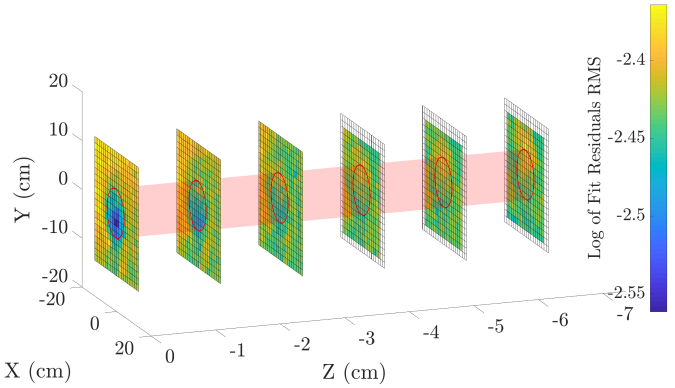

(a) Residuals RMS for Measurement Locations in Experiment A

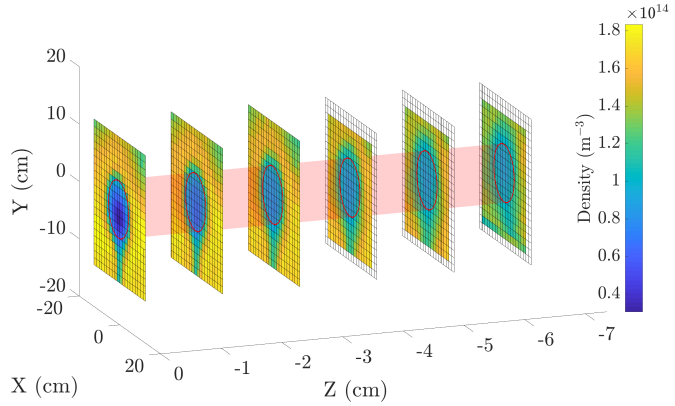

(b) Ion Density Behind a Solid Sphere $V_{\mathrm{sc}} = -1$V (Experiment A)

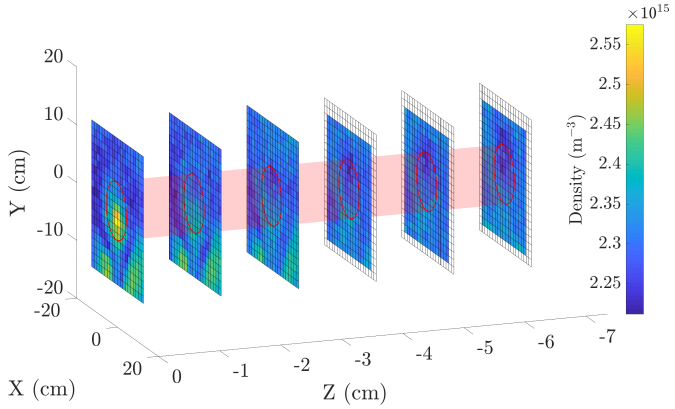

(c) Electron Density Behind a Solid Sphere $V_{\mathrm{sc}} = -1$V (Experiment A)

Fig. 5. Experiment A Data

A. Experiment A

The goal of experiment A is to provide a baseline for the nominal wake behind a spacecraft in LEO. The spherical mock spacecraft shown in Figure 2 is allowed to float at a measured potential of roughly -1 V. The grid size beyond Z = -3cm is reduced due to time constraints for this experiment.

Figure 5a shows the RMS of the fit residuals for each measurement point in experiment A. Note that, for this and other RMS residuals plots, the colorbar has a logarithmic scale, meaning that the RMS values for this experiment are all quite small. This means that, according to the theory described in [24], the plasma parameters collected throughout this experiment should be reasonably accurate. Recall, however, that this RMS value does not indicate which parts of the Langmuir curve are well-fit and which are not. Instead, comparison with previous experiments, simulations, and theoretical work on spacecraft wakes will be applied to better interpret the data. Figure 5b shows the ion density measured across the grid space. The results here indicate a factor of roughly two orders of magnitude between the density of the wake and the ambient. This qualitatively matches previous experimental and simulation data presented in [8] and [11], though the former of these present current rather than plasma parameters. One interesting feature from this plot is that the ceramic post used

to hold the conducting sphere in the plasma flow creates its own wake that can be seen as a perturbation in the plasma on the X = 0 cm line.

The electron density measurements shown in Figure 5c indicate an enhancement in the wake, which is not predicted by previous work and is assumed to be an experimental artifact. The electron density which is determined from the positive voltage end of the Langmuir sweep called the electron saturation region also seems to be fit poorly in the sense of Figure 4c. This could lead to a miscalculation of the electron density resulting in the enhancement seen in the data. Additionally, the lack of differential pumping of the source could allow low-energy ions to penetrate into the wake, potentially resulting in a physical scenario in which more electrons are present in the wake. Finally, the shielding within the wake discussed previously could lead to increased current collection in the positive end of the Langmuir sweep, erroneously implying larger density values.

B. Experiment B

Experiment B was motivated by a desire to understand whether the closing distance of the wake can be shortened by charging the craft negatively with respect to the surrounding plasma. To understand the usefulness of such an technique, consider a docking scenario in which two charged spacecraft are approaching one another in the along-track direction. Reference [27] describes a plasma contactor which ejects plasma to discharge spacecraft. However, if the wake can be made smaller so the ambient plasma envelops the follower craft, the potential difference between the crafts can be lessened without including these additional systems. The -50V potential was chosen because it is large compared to the thermal energy — or relative kinetic energy on orbit — of the plasma, and because spacecraft naturally charge to larger negative voltages than this on orbit [6].

Note that the RMS fit residuals in the wake shown in 6a are much larger than those previous. This results from extremely low plasma density in the wake for this experiment — i.e. most Langmuir sweeps in the wake resemble Figure 4b. While this precludes discussion of wake properties arising from this scenario, it does provide geometric information regarding closure of the wake. This can be seen in Figure 6b.

Contrary to the expected result, charging the spacecraft negative made the closing distance of the wake larger. This is likely because the sheath surrounding the conducting sphere is large, collecting more ions than would a more positively charged object. This hypothesis could not be validated because the Agilent E3633A used to charge negative did not have current resolution small enough to measure the plasma current onto the sphere.

Another interesting result is the ‘deepening’ of the wake. This term is used henceforth to indicate a more significant ion density decrease relative to ambient than that shown in Figure 5b. This is likely because any ions that are able to penetrate into the wake are promptly attracted to the negatively charged sphere and absorbed.

The electron density shown in Figure 6c evidences the data reliability and fitting issues described previously resulting

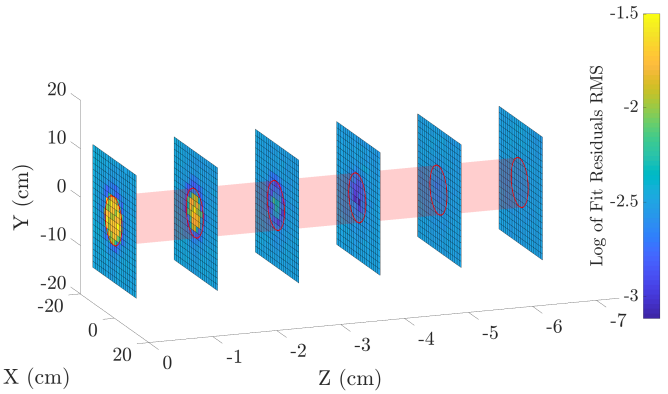

(a) Residuals RMS for Measurement Locations in Experiment B

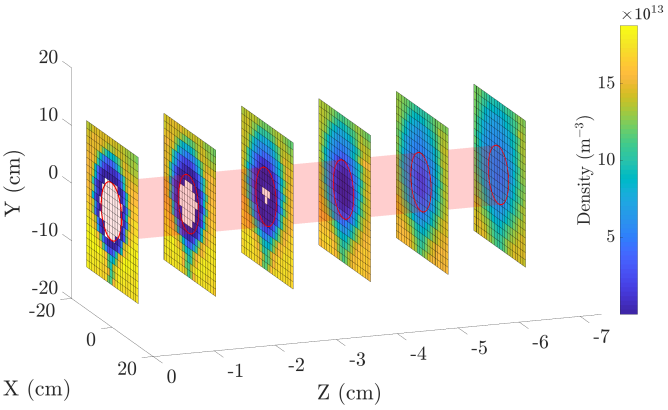

(b) Ion Density Behind a Solid Sphere $V_{sc} = -50$V (Experiment B)

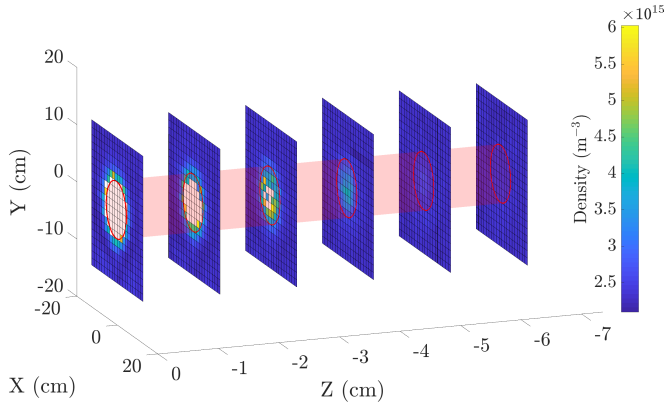

(c) Electron Density Behind a Solid Sphere $V_{sc} = -50$V (Experiment B)

Fig. 6. Experiment B Data

from reaching the floor of the detector and the limit of the Langmuir probe analysis method described by reference [24], respectively. The ambient density matches those shown in Figure 5c. A significant density enhancement is still seen in the few measurements near the wake that were fit well by Equation (1).

C. Experiment C

The ‘enhanced’ wake generated behind a positively charged object is discussed in [28]. Expanding the wake creates a larger

region amenable to electrostatic actuation, so the extent to which this can be accomplished with reasonable charge levels is a subject of interest. As with the previous experiment, the power requirements to hold the conducting sphere at the desire potential could not be measured. However, experiments such as [29] have charged positive by 100s of volts in LEO, so a voltage of 50V should be attainable. The expanded grid shown in Figure 7 was chosen in the hopes of capturing the entirety of the wake for this voltage regime.

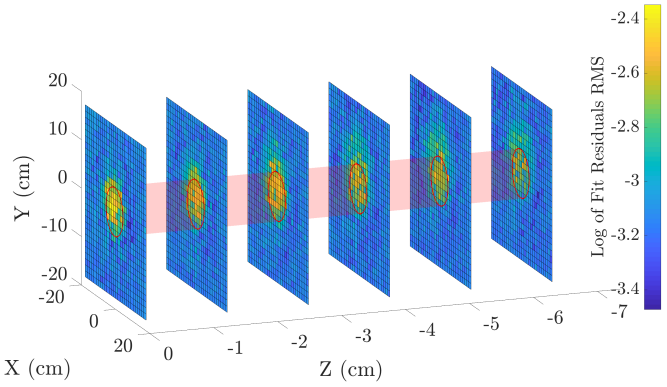

(a) Residuals RMS for Measurement Locations in Experiment C

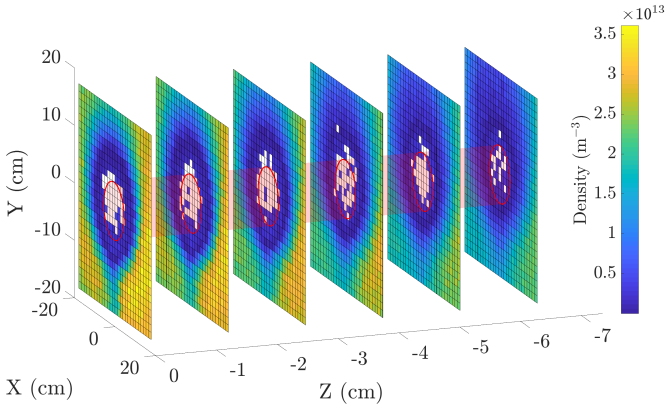

(b) Ion Density Behind a Solid Sphere $V_{sc} = 50$V (Experiment C)

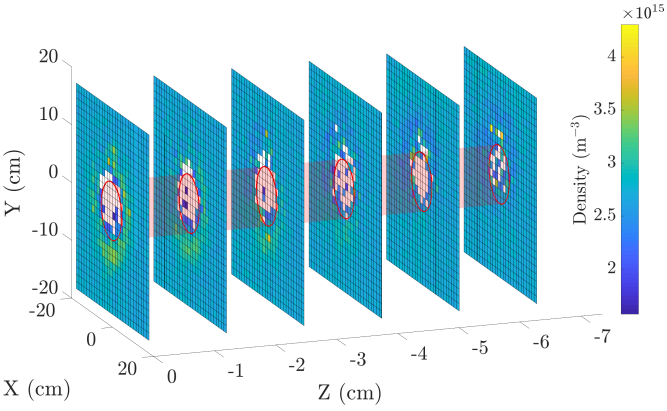

(c) Electron Density Behind a Solid Sphere $V_{sc} = 50$V (Experiment C)

Fig. 7. Experiment C Data

Figure 7a indicates that the general fit quality expressed by the RMS residual values in this experiment should be similar to that in experiment A. However, additional checks on the second derivative of Equation (1) given the fit parameters eliminate data sets that had good RMS values, but do not provide realistic plasma properties.

The wake region indicated by the ion density decreases in Figure 6b is significantly larger for this experiment than those previous. This matches intuition, as the potential on the conducting sphere is about an order of magnitude higher than the expected thermal energy of the ions leaving the source. Note, however, that the out-of-wake ion density shown in Figure 7b is roughly an order of magnitude smaller than those measured in the previous experiments shown in Figures 5b and 6b. This indicates that the 50V charged conducting sphere significantly alters the local plasma environment. Whether this circumstance is representative of what would happen in space or is an artifact of the experiment is unknown. Additional characterization of the source and the plasma flow into JUMBO must be undertaken before these and other questions can be answered. A control experiment will be conducted in which the plasma flow into the chamber is measured without a wake-forming object to disturb the plasma.

Another feature to note in Figure 7b is the extension in the closing distance of the wake. Indeed, it doesn't appear to be closing as is seen in the previous experiments. Rather, it seems that the out-of-wake plasma is thinning and approaching the wake density. As with the X and Y grid dimensions, the Z distance for this experiment was significantly increased compared with the others described in Table I. Visualization of this data is not extremely useful, as the crowding of the contour slices obscures the relevant features. However, the wake shown in Figure 7b does close after roughly 10cm. This is significantly farther than Figures 5b and 6b. This indicates that the wake can indeed be expanded significantly by charging the wake-forming craft positive.

The ambient electron density for this experiment is reminiscent of the experiments described above. As with Figure 6c, the fit and data quality in the wake is low, meaning that the slight density enhancement is likely an artifact of the analysis method.

D. Experiment D

The final experiment is the crux of this investigation. Here, a sparse sphere pictured in Figure 3 is used to create the wake. It has similar dimensions to the charged sphere used previously and is also held at 50V. This object is not a perfect sphere, which creates the interesting wake shape seen in Figure 8b.

As discussed above, the electrostatic actuation techniques require a wake that is large compared to the object within it. Additionally, a larger wake means that the electric field of the charged sphere — whether solid or sparse — is interacting with more of the plasma and exchanging momentum. The goal of experiment C was to determine if a larger wake could be created by charging a craft positive, rather than increasing cross-sectional area and therefore its mass and ballistic coefficient. Experiment D goes a step farther in investigating whether the wake can be expanded by the use of thin, charged structures — which have low mass and cross sectional area. If

this can be accomplished, a craft can enhance its wake without increasing its ballistic coefficient. Additionally, large wakes could be generated behind small, lightweight craft, making electrostatic actuation in LEO more applicable to a range of missions.

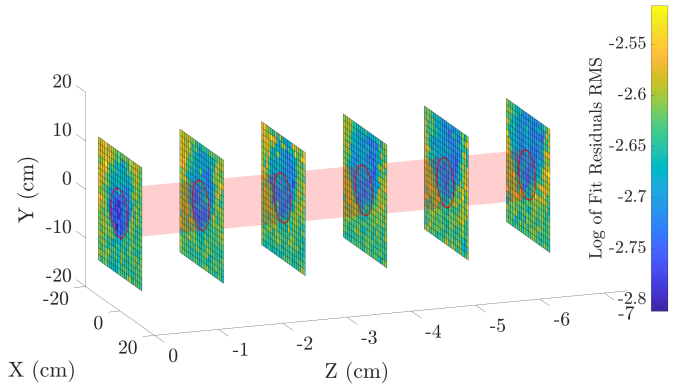

(a) Residuals RMS for Measurement Locations in Experiment D

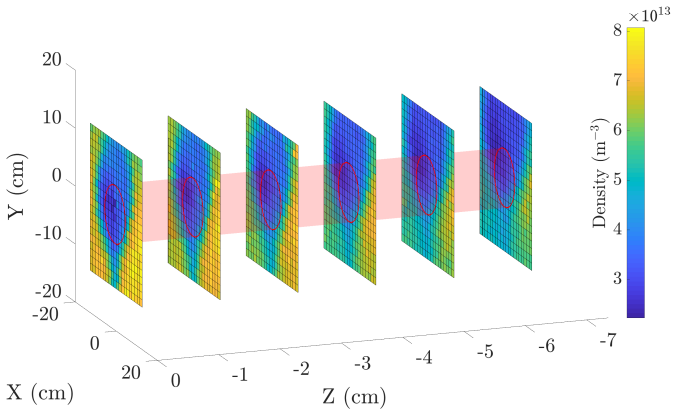

(b) Ion Density Behind a Sparse Sphere $V_{sc} = 50$V (Experiment D)

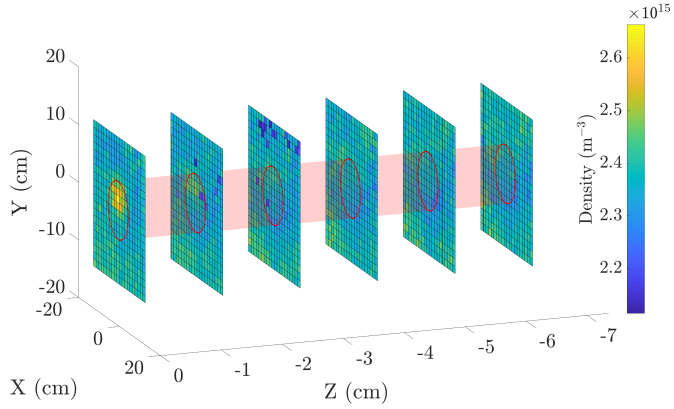

(c) Electron Density Behind a Sparse Sphere $V_{sc} = 50$V (Experiment D)

Fig. 8. Experiment D Data

The fit quality indicated in Figure 8a is quite good overall and provides plasma parameters similar to those seen in previously described experiments. Figure 8b exhibits a similar ion density to that in experiment C, including a wake significantly larger than the diameter of the wake-forming object and with closing distance much larger than those seen in experiments A and B.

A significant difference is seen in the ion density, which is increased relative to experiment C at all points on the grid. This indicates that, while the wake is still large, it is not as deep as when a solid structure is used. Additionally, the charged sparse sphere seems to affect the local plasma environment less than the previous wake-forming object. However, this may not be true of a less-sparse structure. If the cross-sectional area of the sparse sphere were increased — such that in the limit it became a solid sphere once again — the wake would likely look similar to 7b.

Finally, the same density increase is seen in Figure 8c as in the previous experiments. However, the enhancement is much more localized than in Figure 5c. Indeed, the wake shape cannot be seen in Figure 8c as it can be in all previous experiments. This matches the conclusion made with regard to the ion density that the sparse sphere used does not have as significant an effect as a solid object charged to the same voltage.

V. Future Work

A significant challenge when interpreting the results above is the effect of the experiment setup. For this reason, the plasma source and the way the plasma flow expands into the JUMBO chamber will be the subject of future work. A full characterization of the source including the ion energy distribution and plasma expansion in to JUMBO will be undertaken and compared with calibration values and reference [25]. To better measure the ambient plasma, Langmuir probe analysis techniques for a streaming plasma will be employed as described in [30]. Techniques for accurately measuring plasma parameters in the wake will be investigated to provide better estimates of the plasma parameters in this region. Experiments with lower potentials than the $\pm$50V will be conducted to indicate whether the results seen above are artifacts of the limited plasma flow or proximity to chamber walls. Finally, sparse structures of different density, voltage, and geometry will be investigated to determine better means of expanding the wake and thereby the region in which electrostatic actuation can be applied to LEO.

VI. Conclusion

The results above indicate that charging a solid or sparse object positive relative to the plasma potential will expand the wake region. Both the radius of the wake and its closing distance are enhanced in this circumstance. While charging the spherical conductor negative did not appear to decrease the closing distance of the wake, the deepening of the wake seen in Figure 6b indicates an interesting physical phenomenon that could prove advantageous in the application of electrostatic actuation. The plasma parameters in the wake could not be reliably calculated due to the shortcomings of the instrumentation and analysis method, but determination of the size of the wake was still possible. The work presented here provides a solid foundation for the continued investigation of electrostatic actuation in LEO plasma wakes, as well as direction for additional supplementary research related to charged aerodynamics and the relevant applications discussed above.

VII. Acknowledgments

The authors would like to thank Ryan Hoffmann, Dan Engelhart, Dale Ferguson, and Adrian Wheelock for their assistance with both the technical and experimental aspects of this research.

References

[1] J. H. Cover, W. Knauer, and H. A. Maurer, "Lightweight reflecting structures utilizing electrostatic inflation," US Patent 3,546,706, October 1966.

[2] H. Schaub and D. F. Moorer, "Geosynchronous large debris reorbiter: Challenges and prospects," *The Journal of the Astronautical Sciences*, vol. 59, no. 1–2, pp. 161–176, 2014.

[3] H. Schaub and D. Stevenson, "Prospects of relative attitude control using coulomb actuation," *Journal of the Astronautical Sciences*, vol. 60, no. 3, pp. 258–277, 2013.

[4] T. Bennett and H. Schaub, "Touchless electrostatic detumble of a representative box-and-panel spacecraft configuration," in *European Conference on Space Debris*, ESOC, Darmstadt, Germany,, April, 18–21 2017.

[5] ——, "Touchless electrostatic detumbling while tugging large axisymmetric geo debris," in *AAS/AIAA Space Flight Mechanics Meeting*, Williamsburg, VA, Jan. 11–15 2015, paper AAS 15-383.

[6] P. C. Anderson, "Characteristics of spacecraft charging in low Earth orbit," *Journal of Geophysical Research: Space Physics*, vol. 117, no. 7, pp. 1–11, 2012.

[7] D. E. Hastings, "A review of plasma interactions with spacecraft in low Earth orbit," *Journal of Geophysical Research*, vol. 100, no. A8, pp. 14 457–14 483, 1995.

[8] U. Samir, R. Gordon, L. Brace, and R. Theis, "The Near-Wake Structure of the Atmosphere Explorer C (AE-C) Satellite' A Parametric Investigation," *Journal of Geophysical Research*, vol. 84, 1979.

[9] B. E. Troy, E. J. Maier, and U. Samir, "Electron Temperatures in the Wake of an Ionospheric Satellite," vol. 80, no. 7, 1975.

[10] A. R. Martin, "Numerical Solutions to the problem of charged particle flow around an Ionospheric Spacecraft," vol. 22, no. d, pp. 121–141, 1974.

[11] Y. Miyake, C. M. Cully, H. Usui, and H. Nakashima, "Plasma particle simulations of wake formation behind a spacecraft with thin wire booms," *Journal of Geophysical Research: Space Physics*, vol. 118, no. 9, pp. 5681–5694, 2013.

[12] K. R. Svenes and J. Treim, "Laboratory simulation of vehicle-plasma interaction in low Earth orbit," vol. 42, no. 1, 2007.

[13] W. J. Miloch, "Wake effects and Mach cones behind objects," *Plasma Physics and Controlled Fusion*, vol. 52, no. 12, p. 124004, 2010. [Online]. Available: http://stacks.iop.org/0741-3335/52/i=12/a=124004?key=crossref.3c3a6fd90a2da50430e0ec11b243262b

[14] C. Capon, M. Brown, and R. Boyce, "Scaling of plasma-body interactions in low earth orbit," *Physics of Plasmas*, vol. 24, no. 4, p. 042901, 2017.

[15] V. Davis and M. Mandell, "High-voltage interactions in plasma wakes: Simulation and flight measurements from the Charge Hazards and Wake Studies (CHAWS) experiment," *Journal of Geophysical Research*, vol. 104, no. A6, pp. 12,445–12,459, 1999.

[16] S. Sasaki, N. Kawashima, K. Kuriki, M. Yanagisawa, and T. Obayashi, "Vehicle Charging Observed in SEPAC Spacelab-1 Experiment," *Journal of Spacecraft and Rockets*, vol. 23, no. 2, pp. 194–199, 1986.

[17] T. Bennett, D. Stevenson, E. Hogan, and H. Schaub, "Prospects and challenges of touchless electrostatic detumbling of small bodies," *Advances in Space Research*, vol. 56, no. 3, pp. 557–568, 2014. [Online]. Available: http://dx.doi.org/10.1016/j.asr.2015.03.037

[18] H. Schaub and Z. Sternovsky, "Active space debris charging for contactless electrostatic disposal maneuvers," *Advances in Space Research*, vol. 53, pp. 110–118, 2014.

[19] E. A. Hogan and H. Schaub, "Impacts of tug and debris sizes on electrostatic tractor charging performance," *Advances in Space Research*, vol. 55, no. 2, pp. 630–638, 2015.

[20] ——, "General High-Altitude Orbit Corrections Using Electrostatic Tugging with Charge Control," *Journal of Guidance, Control, and Dynamics*, vol. 38, no. 4, pp. 699–705, 2015. [Online]. Available: http://arc.aiaa.org/doi/10.2514/1.G000092

[21] L. A. Stiles, H. Schaub, K. K. Maute, and D. F. Moorer, "Electrostatically inflated gossamer space structure voltage requirements due to orbital perturbations," *Acta Astronautica*, vol. 84, pp. 109–121, 2013. [Online]. Available: http://dx.doi.org/10.1016/j.actaastro.2012.11.007

[22] C. J. Capon, M. Brown, and R. R. Boyce, "Charged aerodynamics of a low earth orbit cylinder," in *AIP Conference Proceedings*, vol. 1786, no. 1, 2016.

[23] R. Cooper and R. Hoffman, "Jumbo space environment simulation and spacecraft charging chamber characterization," Air Force Research Laboratory, Space Vehicles Directorate Kirtland AFB United States, Tech. Rep., 2015.

[24] A. Azooz, "Four free parameter empirical parametrization of glow discharge langmuir probe data," *Review of Scientific Instruments*, vol. 79, no. 10, p. 103501, 2008.

[25] P. Mora, "Plasma expansion into a vacuum," *Physical Review Letters*, vol. 90, no. 18, p. 185002, 2003.

[26] B. Durand de Gevigney, T. Sunn Pedersen, and A. H. Boozer, "Debye screening and injection of positrons across the magnetic surfaces of a pure electron plasma in a stellarator," *Physics of Plasmas*, vol. 18, no. 1, p. 013508, 2011.

[27] I. Katz, B. Gardner, M. Mandell, G. Jongeward, M. Patterson, and R. Myers, "of plasma contactor performance," *Journal of spacecraft and rockets*, vol. 34, no. 6, pp. 824–828, 1997.

[28] S. T. Lai, *Fundamentals of Spacecraft Charging: Spacecraft Interactions with Space Plasmas*. Princeton University Press, 2011.

[29] D. L. Cooke and I. Katz, "Tss-1r electron currents: Magnetic limited collection from a heated presheath," *Geophysical research letters*, vol. 25, no. 5, pp. 753–756, 1998.

[30] S. B. Segall and D. W. Koopman, "Application of cylindrical langmuir probes to streaming plasma diagnostics," *The Physics of Fluids*, vol. 16, no. 7, pp. 1149–1156, 1973.